The 2010 IEEE/RSJ International Conference on
Intelligent Robots and Systems
October 18-22, 2010, Taipei, Taiwan

Enriched Indoor Environment Map Building Using Multi-Sensor Based Fusion Approach

Ren C. Luo, Chun C. Lai and Chin C. Hsiao

Abstract—**Intelligent Service Robot (ISR) has become increasingly noticed because of new devices and novel technologies that make ISR a truly handy human aid in areas like medical care, security patrol, tour guide and edutainment. Therefore, how to provide an applicable map for ISR to autonomously navigate inside a building for task execution becomes an imminent issue. This paper investigates an information enriched map constructed by the environment geometry from laser range finder and the indoor directive signs commonly seen in living/working environment from camera image. To implement this enriched map, multi-sensor fusion techniques are utilized for robust pose and sign estimations. Furthermore, an improved alignment technique is applied to reduce the computational complexity in a single Graph-SLAM process.**

I. Introduction

CONSIDER the actual applications of an intelligent service robot (ISR), it is expected that an ISR will not only autonomously estimate the environment structure but also detect the meaningful symbols or signs in the building it services. For example, an ISR has to locate all the docking stations for recharging itself. For an ISR to lead a customer in the department store to any location such as the toy department or the nearest restroom, it must have the essential recognizing and guiding ability for its service. For this purpose, to carry out an applicable self-localization and map building technique for the indoor service robot becomes important and desirable.

In recent years the sensing and computing technology have made tremendous progress. Various simultaneous localization and mapping (SLAM) techniques have been implemented. The principle of SLAM is derived from Bayesian framework. The EKF-SLAM [1] is based on robot state estimation. However, EKF-SLAM will fail in large environments caused by inconsistent estimation problem from the linearization process [2] [3] [4]. A full SLAM algorithm is using sequential Monte Carlo sampling method to calculate robot state as particle filter [5] [6]. But the technique will grow exponentially with the increase of dimensions of the state space. Another full scan matching method is suitable for the environment reconstruction [7] [8]. But the pose variable will also grow enormously depending on the sampling resolution.

Based on the practical needs of a service robot application in the building, it is desirable to construct an information map autonomously in a unitary SLAM process. This information map consists of geometrical structure of the environment and meaningful sign patterns. This paper investigates a multi-sensor approach to combine the estimation of the sign patterns and a new optimal alignment approach to build a consistent information map. The overall of system architecture is shown in Fig. 2 (a) and some meaningful Patterns of Interest (POI) are defined as in Fig. 2 (b). These patterns are common in any building thus are used in the POI database.

From the system diagram in Fig. 2 (a), the covariance intersection (CI) fusion rule is applied for a more robust criterion on robot pose estimation which is described in section II. Section Ⅲ presents consistent association method and optimal alignment methodology for geometory map building. Section Ⅳ describes POI detection and depth estimation from the stereo camera with Covariance Union (CU) method. The information map building results are demonstrated in section Ⅴ and section Ⅵ is the summary and conclusion.

II. Robot Pose Estimation

A. Pose Estimation from ICP

In 3D shapes registration application, the iterative closest point (ICP) algorithm was successful apply to align two given point data sets. The ICP algorithm was developed by Besl and McKay [9] and the principle works as follows. Let

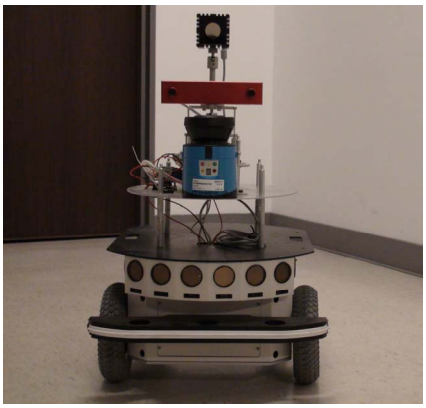

Fig. 1. SICK LMS-100 and Stereo Camera are equipped on the mobile robot platform

Ren C. Luo is with the National Taiwan University, Taipei 10617, Taiwan, (e-mail: renluo@ntu.edu.tw).
Chun C. Lai is with the National Taiwan University, Taipei 10617, Taiwan, (e-mail: cclai@ira.ee.ntu.edu.tw).
Chun C. Hsiao is with the ITRI, Hsinchu 31040, Tawian, (e-mail: hsiao_cc@itri.org.tw).

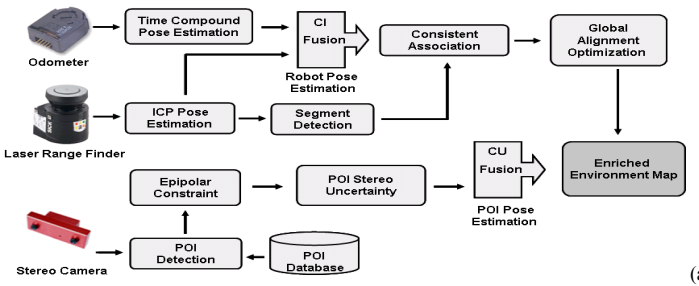

(a)

(b)

Fig. 2. (a) System Flow Diagram Overview (b) Some Meaningful Sign Patterns in the Building

$P_0 = \{p_1,..., p_m\}$ represent the observation point set and $P_r = \{p_1,..., p_n\}$ be the reference point set. The object of the algorithm is to find a geometric transformation to align the observed point P_0 to the reference point set P_r. This transformation is composed of rotation and translation matrix. J. Nieto [10] took the algorithm as an association criterion of EKF-SLAM because ICP algorithm makes the association strengthened using the shape as a gate criterion. In this paper, the ICP result is regarded as a sensor output on pose estimation between two adjacent measurements from laser ranger. The error covariance evolution on the ICP alignment can be derived as follows:

$$z = \{\rho_i, \theta_i\} \quad , \ \rho_i = r_i + \varepsilon$$
$$P_i = [\rho_i \cos\theta_i, \rho_i \sin\theta_i]^T\} \ , \ i = 1...n \qquad (1)$$

where ρ_i is the range data, θ_i is the beam angle and ε is the random error with a Gaussian distribution $N(0,\sigma)$ of the laser range finder. Let I be the error function for ICP algorithm as:

$$I = \sum_i \left\| (R \cdot p_i^k + T) - map\ (R \cdot p_i^k + T, P^{k-1}) \right\| \qquad (2)$$

where k represents the frame or time index and function $map(R \cdot p_i^k + T, P^{k-1})$ maps the data points p_i in frame k into the model points in frame $k-1$. The ICP algorithm always can find out the transform if the error function can be minimized within a threshold, i.e., ICP arrives in a fit solution. Under this constraint, the covariance approximation depends only on the error function I being minimized and the term $\partial^2 I / \partial Z \partial X$ addresses variation of the error function caused by measurement noise ε. Therefore, the covariance of pose transformation is represented as:

$$\text{cov}(X) \cong \left(\frac{\partial^2 I}{\partial x^2}\right)^{-1} \frac{\partial^2 I}{\partial Z \partial X} \text{cov}(Z) \frac{\partial^2 I}{\partial Z \partial X} \left(\frac{\partial^2 I}{\partial X^2}\right)^{-1} \qquad (3)$$

where Z is from laser measurement and X is the pose transformation. In (7), the Cramér–Rao lower bound constraint is proven satisfied [11].

B. Covariance Intersection on Sensor Fusion

The Covariance Intersection (CI) is a data fusion algorithm which takes a convex combination of the means and covariance in the information space. The major advantage of CI is that it permits filter and data fusion to be performed on probabilistically defined estimates without knowing the degree of correlation among those estimates. Consider two different pieces of measurement A and B from different sources. If given the mean and variance: $\mathrm{E}\{\mathrm{A}\} = \mathrm{a}$, $\mathrm{E}\{\mathrm{B}\} = \mathrm{b}$, $\mathrm{var}\{\mathrm{A}, \mathrm{A}\} = \mathrm{P_{aa}}$, $\mathrm{var}\{\mathrm{B}, \mathrm{B}\} = \mathrm{P_{bb}}$, $\mathrm{cov}\{\mathrm{A}, \mathrm{B}\} = \mathrm{P_{ab}}$ Define the estimate Z as a linear combination of A and B where are present the previous estimate of the same target with certain measurement uncertainty. The CI approach is based on a geometric interpretation of the Kalman filter process. The general form of the Kalman filter can be written as:

$$\hat{\mathrm{z}} = \omega_{\mathrm{a}}\mathrm{a} + \omega_{\mathrm{b}}\mathrm{b} \qquad (4)$$

$$\mathrm{P_{zz}} = \omega_{\mathrm{a}}\mathrm{P_{aa}}\omega_{\mathrm{a}}^{\ \mathrm{T}} + \omega_{\mathrm{a}}\mathrm{P_{ab}}\omega_{\mathrm{a}}^{\ \mathrm{T}} + \omega_{\mathrm{b}}\mathrm{P_{ba}}\omega_{\mathrm{b}}^{\ \mathrm{T}} + \omega_{\mathrm{b}}\mathrm{P_{bb}}\omega_{\mathrm{b}}^{\ \mathrm{T}} \qquad (5)$$

where the weights ω_{a} and ω_{b} are chosen to minimize $\mathrm{P_{zz}}$. This form reduces to the conventional Kalman filter if the estimates are independent ($\mathrm{P_{ab}} = 0$). The covariance ellipsoid of CI will enclose the intersection region and the estimate is consistent. CI does not need assumptions on the dependency of the two pieces of information when it fuses them. Given the upper bounds $\mathrm{P_{aa}} - \overline{\mathrm{P}}_{\mathrm{aa}} \geq 0$ and $\mathrm{P_{bb}} - \overline{\mathrm{P}}_{\mathrm{bb}} \geq 0$, the covariance intersection estimate output are defined as follows:

$$\mathrm{z} = \mathrm{P_{zz}}\{\omega_{\mathrm{a}}\mathrm{P_{aa}}^{-1}\mathrm{a} + \omega_{\mathrm{b}}\mathrm{P_{bb}}^{-1}\mathrm{b}\} \qquad (6)$$

$$\mathrm{P_{zz}} = (\omega_{\mathrm{a}}\mathrm{P_{aa}}^{-1} + \omega_{\mathrm{b}}\mathrm{P_{bb}}^{-1})^{-1} \qquad (7)$$

where $\omega_{\mathrm{a}} + \omega_{\mathrm{b}} = 1$, $0 \leq \omega_{\mathrm{a}}, \omega_{\mathrm{b}} \leq 1$

The parameter ω modifies the relative weights assigned to A and B. Different choices of ω_a can be used to optimize the covariance estimate with respect to different performance criteria such as minimizing the trace or the determinant of $\mathrm{P_{zz}}$. In this method, the minimal determinant cost function of $\mathrm{P_{zz}}$ is chosen.

III. CONSISTENT MAP ALIGNMENT

A. Segment Extraction from Laser Measurement

For building a consistent geometry map, the distinctive beacons should be identified and extracted first. Since most of

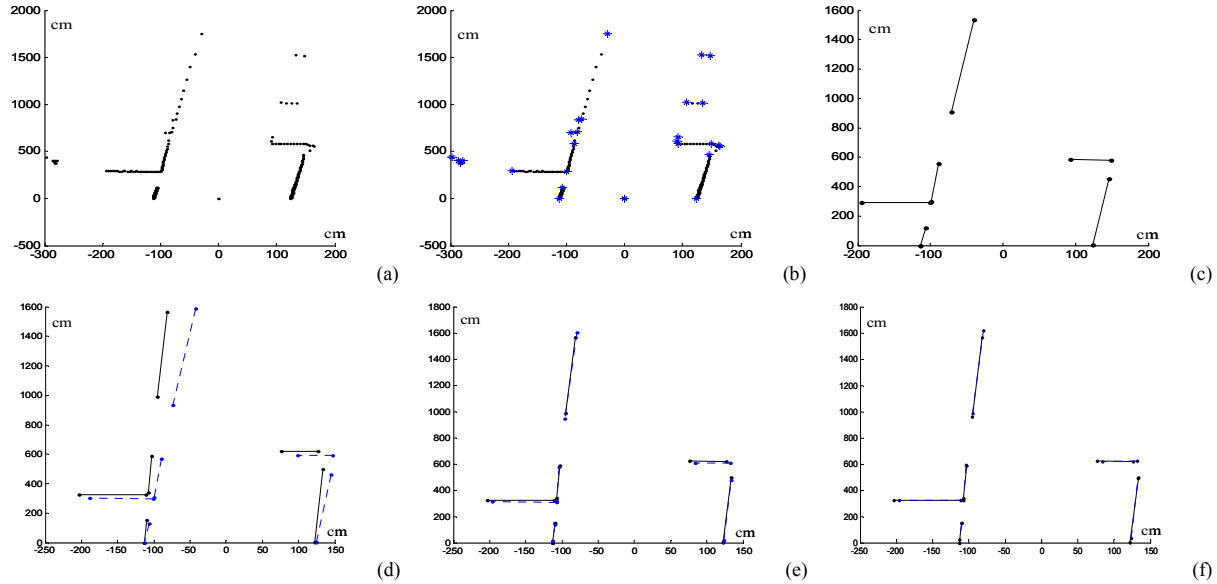

Fig. 3. (a) Laser ranger measurement (b) IEPF result from laser measurement (c) Segment extraction result (d) Segment extraction from two adjacent pose, the solid is model and the dash is new data (e) CI fusion result on adjacent pose variation (f) PSO alignment for eliminating pose residual error

the indoor environment can be efficiently described using polygon segments. The geometry features are defined based on line segments. From each laser ranger measurement $s = \{p_0, p_1, ..., p_{n-1}, p_n\}$, the Iterative End Point Fit (IEPF) [23] method is applied ahead. The IEPF recursively splits S into two subsets $s_1 = \{p_0, ..., p_j\}$ and $s_2 = \{p_j, ..., p_n\}$ while a validation criterion distance d_{max} is satisfied from point p_j to the segment between p_0 and p_n. Through the iteration, IEPF function will return all segment endpoints $\{p_0, p_j\}$ 、 $\{p_j, p_n\}$. However, IEPF only renders cluster points for each segment as candidate. For more precision line segment estimation, a Linear Regression (LR) method is used to estimate the line equation from each segment candidate. Fig. 3 (a) shows the laser measurement. In Fig. 3 (b), the starred points are IEPF results and Fig. 3 (c) shows the segment extraction after LR.

B. Consistent Association and mapping

The objective of the data association is to eliminate the accumulated error from measurements. The issue is focused on having an accuracy link of beacons between current and previous observations. From the physical continuity of robot motion, the adjacent measurement of the environment will have the maximum correlation. Also, the ICP method will reach the maximum matching criterion based on the adjacent measurement. Combining odometer measurements in above section, the robust pose estimation by CI fusion is achieved between the adjacent laser measurements. Fig. 3 (d) shows two adjacent laser scans based on robot center. Fig. 3 (e) shows two adjacent laser scans after the CI fusion result. If there are *r* solid segments in previous frame *n-1* and there are *s* dash segments in current frame *n*. A data association criterion is built based on the adjacent segment distance as below:

$$\begin{aligned} &\text{for segment } j \text{ in segment Set } S \\ &\quad \text{if dist}(seg^{n-1}_{i\in r}, seg^{n}_{j\in s}) < \text{threshold} \\ &\qquad seg^{n}_{j\in s} \text{ is mapping to } seg^{n-1}_{i\in r} \\ &\quad \text{esle} \\ &\qquad seg^{n}_{j\in s} \text{ is a new landmark} \end{aligned} \tag{8}$$

Via the criterion, the global data association will be connected by successive mapping. Furthermore, the global feature will grow up when a new segment beacon is observed. In order to eliminate the residual error accumulated from pose estimation, a global fitness function is generating based on the global association via the association look up table. The fitness function is composed of Euclidean distance between the all segments that associated to the primitive global segments.

$$fitness = \sum_{i=1}^{k} \frac{\left|a_i x_i^1 + b_i y_i^1 + c_i\right| + \left|a_i x_i^2 + b_i y_i^2 + c_i\right|}{\sqrt{a_i + b_i}} \tag{9}$$

where k is the quantity of the segment mapping between the adjacent frames. The a_i , b_i and c_i are the corresponding segment parameters in global frame and (x_i, y_i) are the endpoints which are translated by current robot pose.

C. Pose Alignment Using Particle Swam Optimization

The PSO technique was proposed by Eberhart and Kennedy in 1995 [12] [13] has been widely used in finding solutions for multi-variable optimization problems. Some improvements and applications have also been proposed [14]

[15] [16]. It maintains several particles (each represents a solution) and simulates the behavior of bird flocking to find the final solutions. All the particles continuously move in the search space, toward better solutions, until the termination criteria are met. After certain iterations, the optimal solution or an approximate optimal solution is expected to be found.

When applying the PSO technique, each possible solution in the search space is called a particle, which is similar to a bird's move mentioned above. All the particles are evaluated by a fitness function, with the values representing the goodness degrees of the solutions. The solution with the best fitness value for a particle can be regarded as the local optimal solution found so far and is stored as *pBest* solution for the particle. The best one among all the *pBest* solutions is regarded as the global optimal solution found so far for the whole set of particles, and is called the *gBest* solution. In addition, each particle moves with a velocity, which will dynamically change according to *pBest* and *gBest* . After finding the two best values, a particle updates its velocity by the following equation:

$$V_{id}^{new} = \omega \times V_{id}^{old} + c_1 \times Rand_1() \times (pBest_{id} - x_{id}) + c_2 \times Rand_2() \times (gBest_{id} - x_{id}) \quad (10)$$

where the terms are represented below:

1) V_{id}^{new} :the new velocity of the i-th particle in the d-th dimension in the next generation; V_{id}^{old} :the velocity of the i-th particle in the d-th dimension in the current generation;
2) $pBest_{id}$: the current pBest value of the i-th particle in the d-th dimension; $gBest_{id}$: the current gBest value of the whole set of particles in the d-th dimension;
3) x_{id} the current position of the i-th particle in the d-th dimension;
4) ω : the inertial weight; c_1 : the acceleration constant for a particle to move to its *pBest* ; c_2 : the acceleration constant for a particle to move to the $gBest_{id}$;
5) $Rand_1()$, $Rand_2()$: two random numbers between 0 to 1.

After the new velocity is found, the new position for a particle can then be obtained by the following formula:

$$x_{id}^{new} = x_{id}^{old} + V_{id}^{new} \quad (11)$$

The proposed approach works well to find out the optimal fitness based on beacons alignment. The pose fusion result from odometer and ICP method described in section Ⅲ gives a good initial guess on the optimal search as shown in Fig. 3 (e). Fig. 3 (f) shows the alignment result after PSO, the residual error of robot pose translation is almost eliminated.

IV. Estimation on Pattern of Interest

A. POI detection using SIFT

Recently, the Scale Invariant Feature Transform (SIFT) has emerged as an effective tool in general object recognition, as well as for other machine vision applications [19] [20]. SIFT presents a method for extracting distinctive invariant features from matching images between different views of an object or scene. An important aspect of this approach is that it generates large numbers of features in local region such as location, scale, rotation, magnitude, and orientation in order to record information of key points. Followings are the major stages of computation used to obtain the set of image features:

1) Scale-space extreme detection: The first stage task is to search the potential interest points that are invariant to scale and orientation by repeatedly using a difference of Gaussian function.
2) Key point localization: Key points are selected based on measuring their stability (maximum or minimum) of difference of Gaussian images at each candidate location.
3) Orientation assignment: An orientation is assigned to each key point location based on local image gradient directions in cluttered background.
4) Key point descriptor: These are recorded as a feature vector around each key point by transformation to resist the local shape distortion and change in illumination.

With known paired camera parameters, the SIFT features of POI in the left and right images are matched using the following criteria: disparity constraint, orientation constraint and scale constraint. A POI image is matched by individually comparing each feature from the camera image to the database to look for the maximal match based on Euclidean distance. Fig. 5 (c) in section V shows the SIFT features of a fire extinguisher in database which are matched by the pair of camera images. It is seen that the lines are all horizontal as expected due to the epipolar constraints.

B. Range Estimation from Stereo Vision Constraints

To calculate the distance from a pair of camera, the first step is calibrating the cameras. After calibration, assuming that the cameras are perfectly undistorted, aligned and the two camera's image planes are exactly coplanar with each other. The epipolar constraint reduces to check whether both features are in the same row. However, consider the measurement uncertainty of the feature point in the world due to errors in the image quantization and detection formula. Fig. 4 shows the world coordinates (X , Y , Z) of a feature point can be computed from two matched points in the left and right images as:

$$X = \frac{(c - c_0)b}{d} \quad Y = \frac{(r - r_0)b}{d} \quad Z = \frac{fb}{d} \quad (12)$$

where (r_0, c_0) are the coordinates of the reference image center, (r, c) are the coordinates of the key point in the reference image (the left one), b is the baseline between the

CCD, d is the disparity, and f is the focal length of both cameras. The errors in the variables r, c, and d, are usually modeled as uncorrelated zero-mean Gaussian random variables with the variance σ_c^2, σ_r^2 and σ_d^2. Using the first-order error propagation to approximate the distribution of the variables as multivariate Gaussians, the following covariance matrix can be obtained:

$$\Delta = \begin{pmatrix} \sigma_X^2 & \sigma_{XY}^2 & \sigma_{XZ}^2 \\ \sigma_{XY}^2 & \sigma_Y^2 & \sigma_{YZ}^2 \\ \sigma_{XZ}^2 & \sigma_{YZ}^2 & \sigma_Z^2 \end{pmatrix} = \mathrm{J}\, diag(\sigma_c^2, \sigma_r^2, \sigma_d^2,)\mathrm{J}^{\mathrm{T}} \qquad (13)$$

where **J** is the Jacobian matrix of the functions in (12), and σ_X^2, σ_Y^2, σ_Z^2, σ_{XY}^2, σ_{XZ}^2, σ_{YZ}^2 are the variances and co-variance of the corresponding coordinate variables. Eq. (13), can describe the uncertainty model in the coordinate measurements of the key points on the paired camera system approximately.

C. *Covariance Union Fusion on Visual POI Estimation*

Covariance Intersection represents the general form of the data fusion problem for mean and covariance estimates, but in practice a different fusion format can even be performed. Specifically if there are two pairs of estimation $(\mathrm{P_a}, \mathrm{a})$ and $(\mathrm{P_b}, \mathrm{b})$ which represent covariance and mean to the same real-world object, but the differences between their means is much larger than what can be expected based on their respective error covariance estimates. For example, if we estimate two mean positions with the difference in several metering scale, but their respective covariance indicate each mean is accurate within a few centimeters. Obviously, something is wrong when CI is applying. On the other hand, if it is not possible to prune estimates, then the only alternative is to associate the similar property within a description. The main question is how to achieve this coalescence such that the integrity of the information is maintained. A mechanism called Covariance Union (CU) can be applied under this situation. For example, given n estimations represented by estimates $(\mathrm{P_{a1}}, \mathrm{a_1})$ $(\mathrm{P_{a2}}, \mathrm{a_2})$ . . . $(\mathrm{P_{an}}, \mathrm{a_n})$, CU produces an estimate $(\mathrm{P_u}, \mathrm{u})$ that is guaranteed to be consistent as long as the estimate $(\mathrm{P_{a_i}}, \mathrm{a_i})$ is consistent. This is achieved by guaranteeing that the estimate $(\mathrm{P_u}, \mathrm{u})$ is consistent with respect to each of the estimates. The CU constraint is:

$$\begin{aligned} \mathrm{P_u} &\geq \mathrm{P_{a_1}} + (\mathrm{u} - \mathrm{a_1})(\mathrm{u} - \mathrm{a_1})^T \\ \mathrm{P_u} &\geq \mathrm{P_{a_2}} + (\mathrm{u} - \mathrm{a_2})(\mathrm{u} - \mathrm{a_2})^T \\ &\vdots \\ \mathrm{P_u} &\geq \mathrm{P_{a_n}} + (\mathrm{u} - \mathrm{a_n})(\mathrm{u} - \mathrm{a_n})^T \end{aligned} \qquad (14)$$

The CU optimization has simple linear constraints that are compatible with any generic constrained optimization package. The constraint is applied into a linear matrix inequality (LMI) for a minimum volume ellipsoid

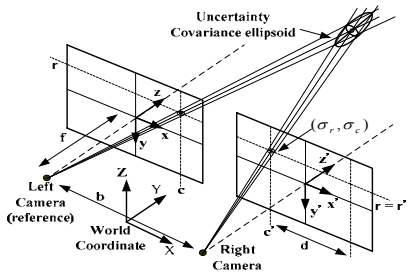

Fig. 4. Stereo Vision Estimation

E_0 containing k given ellipsoids. Each ellipsoid equation with a quadratic functions as:

$$E_i = \{X | X^T A_i X + 2 b_i X + C_i \leq 0\}, i = 0, \ldots, k \qquad (15)$$

The minimum volume can be found by solving the following determinant maximization problems:

Minimize $\log\det A^{-1}$

Subject to :

$$A_0 = A_0^T > 0 \ , \ \tau_i \geq 0$$

$$\begin{bmatrix} A_0 & b_0 & 0 \\ b_0^T & -1 & b_0^T \\ 0 & b_0 & -A_0 \end{bmatrix} - \tau_i \begin{bmatrix} A_0 & b_i & 0 \\ b_i^T & c_i & 0 \\ 0 & 0 & 0 \end{bmatrix} \leq 0 \ , i = 1, \ldots, k \qquad (16)$$

where c_0 is given by $(c_0 = b_0^T A_0^{-1} b_0 - 1)$ [21]. The maxdet-problem is a convex optimization problem. It can consider convex optimization to be a generalization of linear programming which can be solved by several algorithms with efficiency such as in [22].

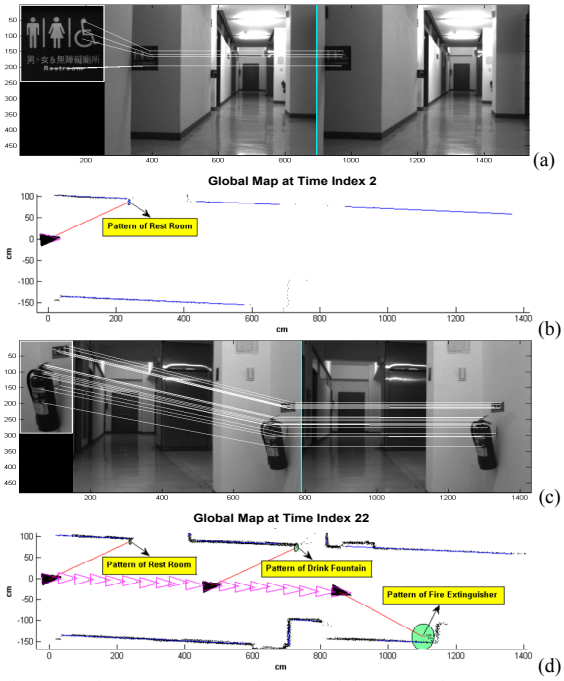

Fig. 5. (a) The sign of restroom is detected (b) Locate the restroom position in global map (c) The fire extinguisher is detected (d) Locate the fire extinguisher in global map

V. Experimental Results

A SICK LMS-100 laser range finder and a paired camera are quipped with robot platform as shown in Fig. 1. In each sampling time index, the odometer, laser measurement and stereo images are compounded and recorded. Applying the consistent alignment methodology described in section Ⅲ, the robot pose can be optimally corrected in global frame after each measurement. Accompanied with the POI detection and estimation from stereo images, the position of POI will also be located in the global map. The experiment environment is a 30m x 30m floor space inside the building. From Fig. 5 (a) to Fig. 5 (d), the part sequences of the map build-up process are demonstrated. When robot is moving forward at time index 2, the sign of restroom is correctly recognized by SIFT constraints as shown in Fig. 5 (a) and the corresponding depth uncertainty is estimated by CU in the global map as shown in Fig. 5 (b). When robot is moving at time index 22, the actual fire extinguisher is recognized as shown in Fig. 5 (c) and the corresponding depth uncertainty is located in the global map as shown in Fig. 5 (d). Finally, when the robot finishes the loop tour, the enriched map of the floor space will be autonomously generated as shown in Fig. 6.

VI. Conclusion

A novel idea is presented in this paper to have an ISR will not only autonomously estimate the environment structure but also simultaneously detect the meaningful symbols or signs in the building it services. The result is an information enriched map which consists of geometry by laser range finder and directive signs from camera, ready for ISR to navigate and service. The experiment result showed the methodologies proposed in this work can construct information enriched indoor 2D map accurately and efficiently.

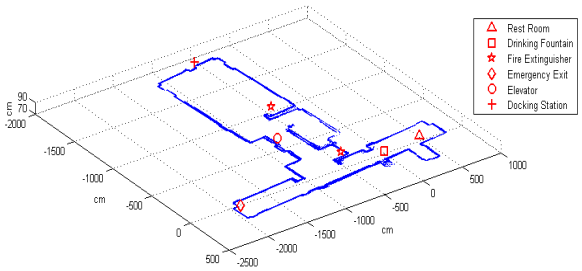

Fig. 6. The complete information map of the floor space

References

[1] H. Durrant-Whyte and T. Bailey, "Simultaneous localization and mapping: part I," *IEEE Robotics & Automation Magazine,* vol. 13, pp. 99-110, 2006.

[2] D. Rodriguez-Losada, F. Matia, and R. Galan, "Building geometric feature based maps for indoor service robots," *Robotics and Autonomous Systems*, vol. 54, pp. 546-558, 2006.

[3] T. Bailey, J. Nieto, J. Guivant, M. Stevens, and E. Nebot, "Consistency of the EKF-SLAM Algorithm," *IEEE/RSJ International Conference on Intelligent Robots and Systems*, 2006, pp. 3562-3568.

[4] H. Shoudong and D. Gamini, "Convergence and Consistency Analysis for Extended Kalman Filter Based SLAM," *IEEE Transactions on Robotics*, vol. 23, pp. 1036-1049, 2007.

[5] M. Montemerlo, S. Thrun, D. Koller, and B. Wegbreit, "FastSLAM: A factored solution to the simultaneous localization and mapping problem," in *Proceedings of the AAAI National Conference on Artificial Intelligence*, 2002, pp. 593-598.

[6] M. Montemerlo, S. Thrun, D. Koller, and B. Wegbreit, "FastSLAM 2.0: An improved particle filtering algorithm for simultaneous localization and mapping that provably converges," in *Proceedings of the International Joint Conference on Artificial Intelligence*, 2003, pp. 1151-1156.

[7] F. Lu and E. Milios, "Globally consistent range scan alignment for environment mapping," *Autonomous Robots*, vol. 4, pp. 333-349, 1997.

[8] D. Borrmann, J. Elseberg, K. Lingemann, A. Nuchter, and J. Hertzberg, "Globally consistent 3D mapping with scan matching," *Robotics and Autonomous Systems*, vol. 56, pp. 130-142, 2008.

[9] P. J. Besl and H. D. McKay, "A method for registration of 3-D shapes," *IEEE Transactions on Pattern Analysis and Machine Intelligence,* vol. 14, pp. 239-256, 1992.

[10] J. Nieto, T. Bailey, and E. Nebot, "Recursive scan-matching SLAM," *Robotics and Autonomous Systems*, vol. 55, pp. 39-49, 2007.

[11] A. Censi, "On achievable accuracy for range-finder localization," *IEEE International Conference on Robotics and Automation,* 2007, pp. 4170-4175.

[12] R. Eberhart and J. Kennedy, "A new optimizer using particle swarm theory," in *Micro Machine and Human Science, 1995. MHS '95., Proceedings of the Sixth International Symposium on*, 1995, pp. 39-43.

[13] J. Kennedy and R. Eberhart, "Particle swarm optimization," in *Proceedings of the IEEE International Conference on Neural Networks*, 1995, pp. 1942-1948.

[14] Y. Shi and R. C. Eberhart, "A modified particle swarm optimizer," *The IEEE International Conference on Evolutionary Programming*, 1998, pp. 69-73.

[15] A. Stacey, M. Jancic and I. Grundy, "Particle swarm optimization with mutation," *The IEEE Congress on Evolutionary Computation,* 2003, pp.1425-1430.

[16] Z. L. Gaing, "Discrete particle swarm optimization algorithm for unit commitment," *The IEEE Power Engineering Society General Meeting*, 2003.

[17] T. Coleman, M. A. Branch, and A. Grace, "Optimization toolbox," *For Use with MATLAB. User's Guide for MATLAB 5, Version 2, Release II*, 1999.

[18] J. C. Lagarias, J. A. Reeds, M. H. Wright, and P. E. Wright, "Convergence Properties of the Nelder-Mead Simplex Method in Low Dimensions," *SIAM Journal of Optimization*, Vol. 9 Number 1, 1998, pp. 112-147.

[19] M. Brown and D. G. Lowe, "Recognising panoramas," *Ninth IEEE International Conference on Computer Vision,* 2003, pp. 1218-1225 vol.2.

[20] D. G. Lowe, "Distinctive image features from scale-invariant keypoints," *International Journal of Computer Vision*, vol. 60, pp. 91-110, 2004.

[21] S. Boyd, L. El Ghaoui, E. Feron, and V. Balakrishnan. Linear Matrix Inequalities in System and Control Theory, volume 15 of Studies in Applied Mathematics. SIAM, Philadelphia, PA, June 1994.

[22] maxdet: Software for Determinant Maximization Problems. User's Guide, Alpha Version – Wu, Vandenberghe, et al. – 1996

[23] G. A. Borges and M. J. Aldon, "Line extraction in 2D range images for mobile robotics," *Journal of Intelligent and Robotic Systems*, vol. 40, pp. 267-297, 2004.